Am J Cancer Res 2020;10(12):4399-4415
www.ajcr.us /ISSN:2156-6976/ajcr0124259

Original Article

The novel potent TEAD inhibitor, K-975, inhibits YAP1/TAZ-TEAD protein-protein interactions and exerts an anti-tumor effect on malignant pleural mesothelioma

Ayumi Kaneda[1,2], Toshihiro Seike[1], Tomohiro Danjo[1], Takahiro Nakajima[1], Nobumasa Otsubo[1], Daisuke Yamaguchi[1], Yoshiro Tsuji[1], Kaori Hamaguchi[1], Mai Yasunaga[1], Yoichi Nishiya[1], Michihiko Suzuki[1], Jun-ichi Saito[1], Rie Yatsunami[2], Satoshi Nakamura[2,3], Yoshitaka Sekido[4,5], Kiyotoshi Mori[1]

[1]R&D Division, Kyowa Kirin Co., Ltd, Shizuoka, Japan; [2]School of Life Science and Technology, Tokyo Institute of Technology, Yokohama, Japan; [3]National Institute of Technology, Numazu College, Shizuoka, Japan; [4]Division of Cancer Biology, Aichi Cancer Center Research Institute, Nagoya, Japan; [5]Division of Molecular and Cellular Oncology, Nagoya University Graduate School of Medicine, Nagoya, Japan

Received October 15, 2020; Accepted November 2, 2020; Epub December 1, 2020; Published December 15, 2020

Abstract: The Hippo signaling pathway regulates cell fate and organ development. In the Hippo pathway, transcriptional enhanced associate domain (TEAD) which is a transcription factor is activated by forming a complex with yes-associated protein 1 (YAP1) or transcriptional coactivator with PDZ-binding motif (TAZ, also called WWTR1). Hyperactivation of YAP1/TAZ, leading to the activation of TEAD, has been reported in many cancers, including malignant pleural mesothelioma (MPM). Therefore, the YAP1/TAZ-TEAD complex is considered a novel therapeutic target for cancer treatment. However, few reports have described YAP1/TAZ-TEAD inhibitors, and their efficacy and selectivity are poor. In this study, we performed a high-throughput screening of a neurofibromin 2 (NF2)-deficient MPM cell line and a large tumor suppressor kinase 1/2 (LATS1/2)-deficient non-small-cell lung cancer cell line using a transcriptional reporter assay. After screening and optimization, K-975 was successfully identified as a potent inhibitor of YAP1/TAZ-TEAD signaling. X-ray crystallography revealed that K-975 was covalently bound to an internal cysteine residue located in the palmitate-binding pocket of TEAD. K-975 had a strong inhibitory effect against protein-protein interactions between YAP1/TAZ and TEAD in cell-free and cell-based assays. Furthermore, K-975 potently inhibited the proliferation of NF2-non-expressing MPM cell lines compared with NF2-expressing MPM cell lines. K-975 also suppressed tumor growth and provided significant survival benefit in MPM xenograft models. These findings indicate that K-975 is a strong and selective TEAD inhibitor with the potential to become an effective drug candidate for MPM therapy.

Keywords: Anti-cancer agent, covalent inhibitor, Hippo pathway, transcriptional enhanced associate domain (TEAD), mesothelioma

Introduction

The Hippo pathway was identified in *Drosophila* as a signaling pathway that regulates cell proliferation and death by suppressing the activation of *Yorkie* [1]. This pathway is evolutionarily conserved, and yes-associated protein 1 (YAP1) and transcriptional coactivator with PDZ-binding motif (TAZ; WWTR1) are homologs of *Yorkie* in mammals [2, 3]. The Hippo pathway regulates organ development, tissue homeostasis, and tumorigenesis by controlling the activation status of YAP1/TAZ [4].

Major upstream molecules of the Hippo pathway, such as *neurofibromin 2* (*NF2*; *Merlin*), *mammalian sterile 20-like kinase 1/2* (*MST1/2*), and *large tumor suppressor kinase 1/2* (*LATS1/2*), are tumor suppressor genes whereas *YAP1* and *TAZ* are oncogenes. One of the most well-known transcription factors of this pathway is transcriptional enhanced associate domain (TEAD), which binds to its transcriptional coactivator, YAP1 or TAZ, to form a transcription complex [5]. NF2 activates MST1/2, which activates LAST1/2. Activated LATS1/2 phosphorylates YAP1/TAZ, and the phosphorylated YAP/

TAZ is localized in the cytoplasm or degraded in a ubiquitin-dependent manner. Therefore, the upstream molecules of this pathway have a critical role in suppressing the transcriptional activity of the YAP1/TAZ-TEAD complex.

Pobbati et al. reported that TEAD has a hydrophobic pocket that can be accessed by small molecules (a "druggable pocket") in the YAP1-binding domain (YBD) [6]. In mammals, there are four family members, TEAD1, TEAD2, TEAD3, and TEAD4. The DNA binding domain and YAP1/TAZ-binding domain are highly conserved in *Scalloped* (*Sd*; a homolog of TEAD) in *Drosophila* and TEAD1-4 in mammals [7, 8]. In addition, TEAD undergoes auto-palmitoylation in the hydrophobic pocket in both *Drosophila* and mammals [9]. Palmitate binds to the evolutionarily conserved Cys residue in the hydrophobic pocket of TEAD, which is also called the "palmitate-binding pocket" (PBP). Palmitoylation increases the stability of the TEAD protein and increases its affinity with YAP1/TAZ [9, 10]. Accordingly, the modification of Cys-palmitoylation is considered to affect the transcriptional activity of the YAP1/TAZ-TEAD complex. One of the most studied genes transcribed by the YAP1-TEAD complex is *connective tissue growth factor* (*CTGF*) [11]. Thus, its transcription level is used as an indicator of YAP1-TEAD activity.

In some cancers, such as malignant mesothelioma, ovarian cancer, and cholangiocarcinoma, the YAP1/TAZ-TEAD complex is often hyper-activated or over-expressed, leading to cancer progression [12-18]. This hyper-activation is commonly induced by the alteration of genes upstream in the Hippo pathway. In malignant mesothelioma patients in particular, 40%-50% of tumors had a mutation or deficiency in NF2, <25% had an MST1 or LAST1/2 mutation or deficiency, and 70% had a high expression of YAP1 [19, 20]. The hyper-activation of the YAP1/TAZ-TEAD complex contributes to the enhancement of cell proliferation, metastasis, epithelial-to-mesenchymal transition (EMT), and cancer stem cell maintenance in tumor cells [21, 22].

In malignant mesothelioma, the first-line therapy is a combination of pemetrexed (PEM) and cisplatin (CDDP). Although nivolumab, an anti-human programmed cell death-1 (PD-1) monoclonal antibody, was approved as second-line therapy in 2018 [23, 24], the objective response rate of monotherapy with nivolumab is only 19%. Therefore, there is still a high unmet medical need in malignant mesothelioma. Accordingly, the YAP1/TAZ-TEAD complex is now considered an effective therapeutic target for malignant mesothelioma.

Drug development targeting the YAP1/TAZ-TEAD complex has been attempted worldwide, and some inhibitors of YAP1/TAZ-TEAD have been reported. For example, verteporfin was the first small molecule to inhibit the protein-protein interaction (PPI) between YAP1 and TEAD by binding to the WW domain of YAP1 [25]. Furthermore, Inventiva, the General Hospital Corporation and Vivace Therapeutics recently reported a YAP1-TEAD inhibitor [26, 27]. Other than small-molecule inhibitors, vestigial-like family member 4 (VGLL4) competes with YAP1 to bind to TEAD, and a VGLL4-mimicking peptide termed Super-TDU was developed as an inhibitor of YAP1-TEAD PPI [28]. However, none of these inhibitors have sufficient selectivity towards TEAD and/or potency to exert an anti-tumor effect *in vivo*.

In this study, we performed high-throughput screening of our chemical library to discover a novel inhibitor of the YAP1/TAZ-TEAD transcriptional complex. Then, we successfully identified K-975 as a new pan-TEAD inhibitor with strong activity and high selectivity. The mechanism of action and anti-tumor effect of K-975 *in vitro* and *in vivo* was investigated using human malignant pleural mesothelioma (MPM) cell lines. Malignant mesothelioma often has a mutation or deficiency in the CDKN2A gene [29], which reduces the expression of $p16^{INK4a}$, a suppressor of CDK4/6, and induces abnormal cell cycle regulation. Therefore, CDK4/6 inhibitors are considered effective for cases of CDKN2A mutation/deficiency [30]. We also investigated the efficacy of a combination of K-975 and the CDK4/6 inhibitor palbociclib.

Materials and methods

Cells and culture conditions

Several human MPM cell lines were used in this study. NCI-H226 (#CRL-5826), NCI-H2052 (#CRL-5915), NCI-H28 (#CRL-5820), and NCI-H2452 (#CRL-5946) were purchased from American Type Culture Collection (ATCC, Manassas, VA, USA). MSTO-211H (#ACC390)

was purchased from Deutsche Sammlung von Mikroorganismen und Zellkulturen GmbH (DSMZ, Braunschweig, Germany). Y-MESO-9, Y-MESO-14, Y-MESO-26B, Y-MESO-27, Y-MESO-28, and Y-MESO-30 were established at the Aichi Cancer Center Research Institute. These cell lines were cultured in RPMI 1640 with 10% (v/v) fetal bovine serum (FBS). HMMME (RCB-0819) was purchased from Riken BioResource Research Center (Ibaraki, Japan) and cultured in F12 Medium with 15% (v/v) FBS. Mero-14 (#09100101) and Mero-25 (#09100102) were purchased from Dainippon Sumitomo Pharma (Osaka, Japan). Mero-14 and Mero-25 were cultured in F10 Medium with 10% (v/v) FBS. The human non-small-cell lung cancer (NSCLC) cell line, NCI-H661 (#HTB-183, ATCC) was cultured in RPMI 1640 with 10% (v/v) FBS.

The culture conditions were 37°C and 5% CO_2. All cell lines from ATCC and DSMZ were authenticated by a short tandem repeat assay at the Japanese Collection of Research Bioresources (Osaka, Japan). Mycoplasma infection was excluded by MycoAlert Mycoplasma Detection Kit (Lonza, Tokyo, Japan).

Test articles

K-975 was synthesized by Kyowa Kirin (Tokyo, Japan). For PEM, Alimta Injection 100 mg was purchased from Nippon Eli Lilly (Hyogo, Japan). For CDDP, Randa Injection 50 mg/100 mL Formulation was purchased from Nippon Kayaku (Tokyo, Japan). For folic acid, Foliamin Powder 100 mg/g was purchased from Nippon Pharmaceutical (Tokyo, Japan). Palbociclib (HY-5076) was purchased from MedChemExpress (Monmouth Junction, NJ, USA).

siRNAs

For YAP1 knockdown, si-YAP1-1 (#HSS115942; Thermo Fisher Scientific, Tokyo, Japan), si-YAP1-2 (#HSS115944; Thermo Fisher Scientific), and si-YAP1-3 (#S102662954; QIAGEN, Venlo, Netherlands) were used. For TEAD knockdown, TEAD1 siRNA (#S13961), TEAD2 siRNA (#S16076), TEAD3 siRNA (#S13968), and TEAD4 siRNA (#S13965) were used. For negative controls, Control siRNA Med GC #3 (#12935-113), and Negative control siRNA (#4390846) were used. TEAD siRNAs and negative control siRNAs were purchased from Thermo Fisher Scientific.

Reporter assay

A DNA fragment including the CTGF prompter region was amplified using specific primers (sense primer: 5'-GGTCCGGCTAGCATTCTATTTG-GTGCTGGAAA-3', anti-sense primer: 5'-GAATT-AAAGCTTGGGGCGGGCGGCCCGAGGCTTTTA-TA-3') and PrimeSTAR HS polymerase (Takara Bio, Shiga, Japan). The NQO1 ARE element (hARE), used as a NRF2 response element (5'-GTGACTCAGCACCCGTGACTCAGCACCCGTGAC-TCAGCACCCGTGACTCAGCA-3'), was synthesized by Takara Bio. These DNA fragments were cloned into a pGL4.27 vector. The pGL4.27-CTGF plasmid was transfected into NCI-H2052 and NCI-H661 cells. For a counter-screen, the pGL4.27-NRF2 plasmid was transfected into NCI-H661 cells. Hygromycin was then added to the cells to ensure stable clone selection.

A single clone with high reporter activity was selected. NCI-H2052/CTGF-Luc cells, NCI-H661/CTGF-Luc cells, and NCI-H661/NRF2-Luc cells were seeded into 384-well white plates. The next day, the compounds were added and incubated for 24 h, or siRNAs were reverse transfected by RNAiMAX (Thermo Fisher Scientific) and incubated for 48 h. After incubation, Steady Glo reagent (Promega, Madison, WI, USA) was added to the cells, and the reporter activity was measured by TopCount NXT (PerkinElmer, Waltham, MA, USA).

Halo-tag pull-down assay

YAP1-HaloTag human ORF in pFN21A (FHC-10458; or Halo-YAP) and TAZ-HaloTag human ORF in pFN21A (FHC00346; or Halo-TAZ) were purchased from Promega. Cells were then transfected with Halo-YAP or Halo-TAZ by FuGENE HD Transfection Reagent (Promega). The next day, the cells were treated with compounds. After 24 h, the cells were collected and lysed using Mammalian Lysis Buffer (Promega) with a protease inhibitor cocktail (Sigma Aldrich, St. Louis, MO, USA). Each sample (1 mg) was added to HaloLink Resin (Promega) and incubated overnight at 4°C. The next day, the resin was washed several times and then boiled with sodium dodecyl sulfate (SDS) at 95°C for 5 minutes to elute proteins. After elution, the supernatants were collected and used for SDS-polyacrylamide gel electrophoresis (SDS-PAGE) and immunoblotting analyses.

Table 1. Statistics for X-ray crystallographic data collection and refinement

	TEAD1-YBD/K-975
PDB ID	7CMM
Data collection	
X-ray source	SLS X06DA
Space group	$P2_12_12$
Cell dimensions	
a, b, c (Å)	147.99, 151.81, 67.53
α, β, γ (°)	90, 90, 90
Resolutions (Å)	49.33-3.50 (3.83-3.50)
R_{pim} (%)	12.9 (75.8)
Mean I/σ (I)	8.0 (1.3)
$CC_{1/2}$	0.989 (0.614)
Completeness (%)	99.7 (99.7)
Multiplicity	18.6 (19.5)
Refinement	
Resolution (Å)	10.00-3.50 (3.68-3.50)
Number of reflections	18,731 (2,508)
R_{work}/R_{free} (%)	23.3/28.3 (37.6/40.6)
Number of atoms	
Protein	6,394
Ligand	80
Water	4
Mean B value	
Protein	91.5
Ligand	89.5
Water	52.1
RMSD	
Bond lengths (Å)	0.003
Bond angles (°)	0.694
Ramachandran plot	
Favored (%)	98.1
Allowed (%)	1.9
Disallowed (%)	0.0

Values in parentheses are for the highest resolution shell. TEAD, transcriptional enhanced associate domain; YBD, yes-associated protein 1-binding domain; PBD, Protein Data Bank; RMSD, Root Mean Square Deviation.

Preparation of recombinant TEAD1-YBD protein

TEAD1-YBD (amino acids 209-426) fused with an N-terminal GST-tag followed by thrombin and TEV protease cleavage sites was expressed in *Escherichia coli* BL21 (DE3). GST-fused TEAD1-YBD protein was purified by batch affinity chromatography with Glutathione Sepharose 4B (GE Healthcare, Chicago, IL, USA) and size-exclusion chromatography (SEC) with HiLoad 26/600 Superdex 200 pg (GE Healthcare). GST-fused proteins were enzymatically cleaved by biotinylated thrombin (Millipore, Billerica, MA, USA) overnight at 4°C. Thrombin protease and the cleaved GST-tag were then removed by passage through Strept-Tactin Superflow Plus (QIAGEN) and Glutathione Sepharose 4B resin. TEAD1-YBD protein was finally purified by SEC with HiLoad 26/600 Superdex 200 pg, concentrated to 7-10 mg/mL, and stored at -80°C for further use.

Crystallography

Before crystallization, TEAD1-YBD was mixed with K-975 at a 2:1 molar ratio. TEAD1-YBD/K-975 co-crystals were obtained using the sitting drop vapor-diffusion method at 4°C by mixing TEAD1-YBD/K-975 and an equal volume of reservoir solution containing 0.1 mol/L Bis-Tris (pH 5.5-6.5), 0.8-1.4 mol/L ammonium sulfate, and 1.0% (w/v) PEG3350. Diffraction-grade co-crystals were obtained by microseeding. The co-crystals were cryoprotected by immersion in reservoir solution supplemented with 30% (v/v) glycerol and flash cryocooled in liquid nitrogen. X-ray diffraction data were collected at the beamline X06DA of the Swiss Light Source (Paul Scherrer Institute, Villigen, Switzerland) and processed using *XDS* [31]. The co-crystals belonged to the space group $P2_12_12$ with the following unit cell parameters: a = 148.0 Å, b = 151.8 Å, and c = 67.5 Å. The structure was determined by the molecular replacement method with *MOLREP* [32] in the *CCP*4 [33] packages using the known TEAD1-YBD structure in the TEAD1-YBD/YAP1 peptide (YAPpep) complex (PDB ID: 3KYS, chain A) as a search model and refined using *REFMAC*5 [34] and *COOT* [35]. *CCP*4*MG* [36] was used to generate structural drawings. The crystallographic statistics are shown in **Table 1**.

Surface plasmon resonance (SPR) assay

A YAPpep corresponding to 50-100 amino acid residues of YAP1 and biotinylated YAPpep (bio-YAPpep) were synthesized by SCRUM Inc. (Tokyo, Japan). The sequences were as follows: YAPpep (AGHQIVHVRGDSETDLEALFNAVMNPKTANVPQTVPMRLRKLPDSFFKPPE) and bio-YAPpep (biotin-GGGSGGGSAGHQIVHVRGDSETDLEALFNAVMNPKTANVPQTVPMRLRKLPDSFFKPPE). Bio-YAPpep (5 μg/mL) was immobilized on a Series S SA chip (GE Healthcare) at 196.8 RU

following the biotin capture method of the immobilization wizard. TEAD1-YBD protein was diluted with HBS-N (GE Healthcare) to 1 μmol/L and incubated with K-975 or YAPpep for 3 h at room temperature. After incubation, HBS-EP+ (GE Healthcare) was added before measurement using a Biacore T100 (GE Healthcare). The samples were run at a flow rate of 10 μL/min, with 60 sec of contact time and 600 sec of dissociation time. Regeneration was performed with Glycine-HCl (pH 3.0) and Glycine-HCl (pH 2.5) at a flow rate of 30 μL/min for 30 sec.

Auto-palmitoylation assay

TEAD1-YBD (1 μmol/L) and the compounds were incubated in HBS containing 20 mmol/L HEPES-NaOH (pH 7.4) and 150 mmol/L NaCl at room temperature for 1 h. After incubation, 5 μmol/L of palmitoyl-alkyne CoA (Pal Alk-CoA) (Cayman Chemical, Ann Arbor, MI, USA) was added and incubated at room temperature for 2 h. The samples were then mixed with 0.5% SDS. Cy3-picoyl azide (50 μmol/L) (Click Chemistry Tools, Scottsdale, AZ, USA), BTTAA (200 mmol/L), $CuSO_4$ (0.4 mmol/L), and ascorbic acid (5 mmol/L) were added to the SDS-treated samples, and a click reaction was performed at room temperature for 1 h in the dark. After the click reaction, the samples were desalted using Zeba desalting columns and separated by SDS-PAGE. Gels were fixed with 50% MeOH/5% acetic acid and washed with ultrapure water. Fluorescent images of the gels were photographed using an Amersham imager AI600 (GE Healthcare).

SDS-PAGE and immunoblotting analyses

Cells were seeded into 6-well plates or 10-cm dishes. When the cells reached sub-confluency, they were collected and lysed using NP40 lysis buffer (Thermo Fisher Scientific) with a protease inhibitor cocktail (Sigma Aldrich). Proteins in the cell lysate were detected by a standard western blotting procedure using the following antibodies: anti-TEAD1 antibody (LifeSpan BioSciences, Seattle, WA, USA), anti-TEAD4 antibody (Abcam, Cambridge, UK), anti-YAP1 antibody (Cell Signaling Technology), anti-TAZ antibody (Cell Signaling Technology, Danvers, MA, USA), anti-NF2 antibody (Cell Signaling Technology), anti-β-actin antibody (Sigma Aldrich), anti-rabbit IgG, HRP-Linked Whole Ab Donkey (GE Healthcare), and anti-mouse IgG, HRP-Linked Whole Ab Sheep (GE Healthcare).

Cell proliferation assay

Cells were seeded into 96-well plates. The next day, the compounds were added and incubated for 144 h. After 144 h incubation, Cell Counting Kit-8 reagents (Dojindo Molecular Technologies, Rockville, MD, USA) were added to the cells and cultured for 2 to 3 h. The differences in the absorbance between 450 nm and 690 nm ($A = A_{450} - A_{690}$) were measured using a SpectraMax 340PC system (Molecular Devices, San Jose, CA, USA).

Real-time reverse transcription-polymerase chain reaction (RT-PCR)

Cells were seeded into 6-well plates. The next day, the compounds were added and incubated for 24 h, or siRNAs were reverse transfected by RNAiMAX and incubated for 48 h. Subsequently, total RNA extraction from cells was performed using a Maxwell 16 Instrument (Promega) and Maxwell 16LEV Simply RNA Cells Kit (Promega). cDNA preparations were performed using a SuperScript VILO cDNA synthesis kit (Thermo Fisher Scientific). For quantitative real-time PCR, Platinum SYBR-Green qPCR SuperMix-UDG with ROX (Thermo Fisher Scientific) was used. The evaluated genes were *CTGF*, *insulin-like growth factor binding protein-3* (*IGFBP3*), *natriuretic peptide B* (*NPPB*), and *F-box protein-32* (*FBXO32*). *Glyceraldehyde 3-phosphate dehydrogenase* (*GAPDH*) was used as a housekeeping gene. The transcript levels were determined using ABI Realtime PCR 7900HT (Thermo Fisher Scientific) or QuantStudio5 real-time PCR systems (Thermo Fisher Scientific). The primer sets used in RT-PCR are shown in **Table 2**.

Measurement of the anti-tumor effect in subcutaneous (s.c.) transplant mouse models

All animal studies were performed in accordance with the Standards for Proper Conduct of Animal Experiments at Kyowa Kirin under the approval of the company's Institutional Animal Care and Use Committee (protocol number: APS 14J0133). Kyowa Kirin is fully accredited by the Association for the Assessment and Accreditation of Laboratory Animal Care, International.

Table 2. Primer sets used in this study

Gene	Sequence
GAPDH	Forward: 5'-CCACATCGCTCAGACACCAT-3'
	Reverse: 5'-GCAACAATATCCACTTTACCAGAGTTAA-3'
YAP1	Forward: 5'-CTTTGATCTTACGATGCCCTCT-3'
	Reverse: 5'-CAATGCTACCCAATACAACCAA-3'
CTGF	Forward: 5'-CGATTAGACTGGACAGCTTGTG-3'
	Reverse: 5'-TGGTGTTCAGAAATTGAGGCTA-3'
IGFBP3	Forward: 5'-GATCCCTCAACCAAGAAGAATG-3'
	Reverse: 5'-TATAGGTTCCCAGAGTGCCCTA-3'
NPPB	Forward: 5'-CTCCTGCTCTTCTTGCATCTG-3'
	Reverse: 5'-GGACTTCCAGACACCTGTGG-3'
FBXO32	Forward: 5'-TCCCAGACAACCTGACCTATC-3'
	Reverse: 5'-GGGCAGAACTCTTTCCTTCTT-3'

K-975 was suspended in 0.5% methylcellulose 400 solution (MC400) (Fujifilm Wako Pure Chemical, Osaka, Japan). SCID mice (C.B17/Icr-scid/scidJcl, male, 5 weeks-old) were obtained from CLEA Japan. The mice were subcutaneously injected into the right flank with 5×10^6 NCI-H226 cells in PBS containing 50% (v/v) BD Matrigel basement membrane matrix (BD Biosciences, San Jose, CA, USA) or 5×10^6 MSTO-211H cells in PBS containing 50% (v/v) BD high-concentration Matrigel basement membrane matrix (BD Biosciences). When the tumor volumes reached 100-200 mm^3, the mice were divided into groups of five and treated with K-975 twice a day for 14 days by oral administration. For comparison, PEM and CDDP were also administered.

To evaluate the anti-tumor effect of K-975 combined with the CDK4/6 inhibitor palbociclib, mice were orally administered K-975 (100 mg/kg, twice a day, daily) or palbociclib (150 mg/kg, once a day, daily) alone or in combination. For palbociclib, 50 mmol/L lactate buffer (pH 4) was used as a vehicle. The tumor volumes and body weights of mice were measured every 3-4 days.

The tumor volumes on day 15 (for monotherapy studies) or day 21 (for the combination study) were compared statistically between the vehicle- and compound-treated groups. For monotherapy studies, a one-way analysis of variance (ANOVA) followed by William's test was used. For the combination study, a one-way ANOVA test followed by Tukey's test was used. Statistical analyses were carried out using SAS software (Release 9.4, SAS Institute, Cary, NC, USA). For all statistical analyses, $P < 0.05$ was considered statistically significant.

For the analysis of YAP1-TEAD signaling in xenograft tumors, mice with tumor volumes of 200-600 mm^3 were divided into groups of five and administered K-975 twice a day for 3 days. Sixteen hours after the last administration, the tumors were collected and frozen in liquid nitrogen. Total RNA was extracted using TRIzol reagent (Thermo Fisher Scientific) and a Maxwell 16LEV Simply RNA Tissue Kit (Promega). For cDNA preparation and RT-PCR, the same method was used as for the *in vitro* analysis.

Measurement of survival in an orthotopic transplant mouse model

Nude mice (BALB/cAJcl-nu/nu, male, 6 weeks-old) were obtained from CLEA Japan (Tokyo, Japan). On day 0, 1×10^6 NCI-H226 cells in PBS containing 50% (v/v) BD Matrigel basement membrane matrix (BD Biosciences) were injected into the thoracic cavity of the mice through a space between the ribs. At 13 days after the transplantation, mice were weighed and divided into four groups by body weight (10 mice/group). The mice were then administered K-975 (300 mg/kg, twice a day) or chemotherapy (PEM and CDDP) either alone or in combination. The body weights of mice were measured every 3-5 days, and daily measurements were started once weight loss was 15% compared with that on day 1. The blood oxygenation level (partial pressure of oxygen in blood, SpO_2) was also monitored daily in mice with >15% body weight loss using a small-animal experimental pulse oximeter (PhysioSuite; Hakubatec Lifescience Solutions, Tokyo, Japan), with measurements made three times at the femur. Mice with >25% body weight loss from day 1 or SpO_2 <75% were considered dead.

A survival curve was generated using JMP software (version 14.2; SAS Institute). Differences in survival between groups were analyzed by Log-rank test using SAS software (Release 9.4; SAS Institute). For multiple comparisons, Bonferroni's correction was applied, with $P<0.017$ considered statistically significant. The effect of drug administration on the growth of intrathoracic tumors was evaluated

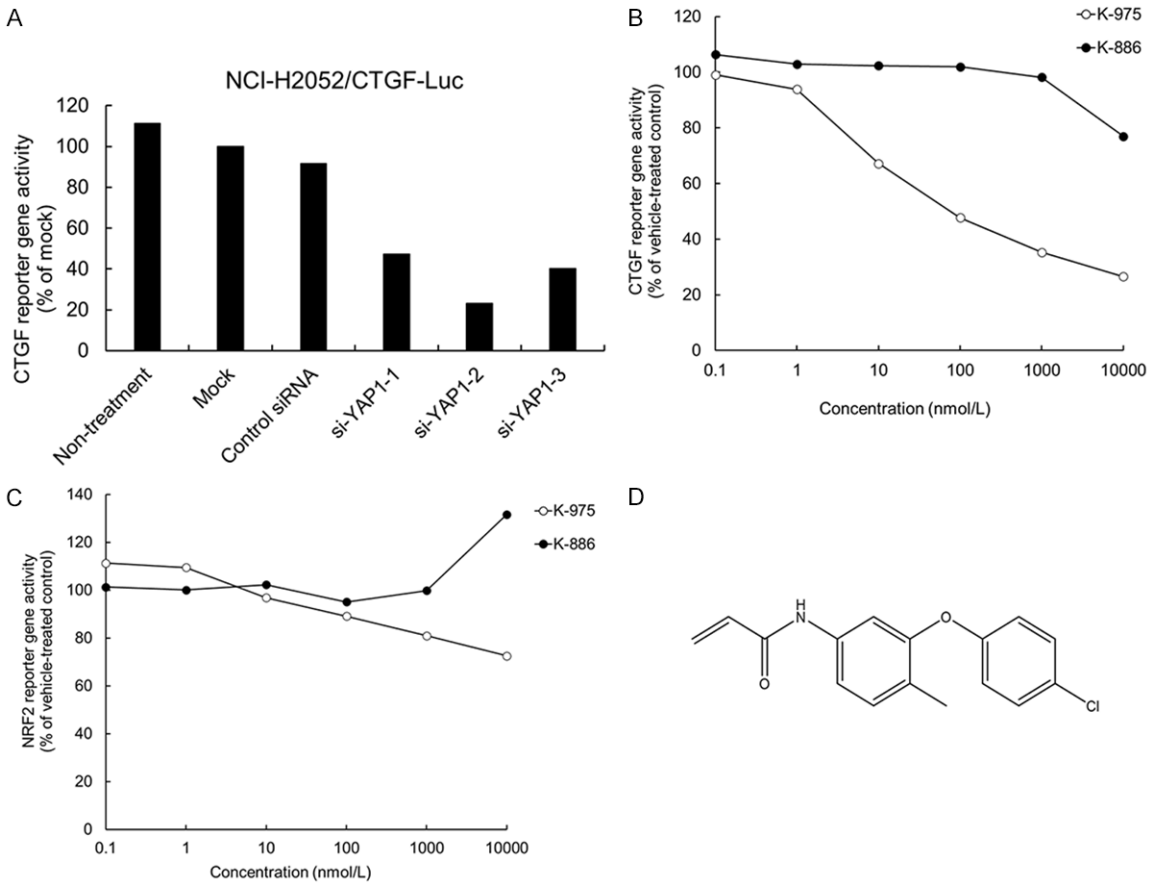

Figure 1. The chemical structure and inhibitory activity of K-975 against yes-associated protein 1 (YAP1)-transcriptional enhanced associate domain (TEAD) signaling. A. YAP1 siRNA inhibited CTGF reporter gene activity in NCI-H661/CTGF-Luc cells. The cells were incubated with si-YAP1-1, si-YAP1-2, or si-YAP1-3 for 48 h, and the luciferase activity was measured. B and C. K-975, but not K-886, a derivative of K-975 with an acrylamide structure, selectively inhibited CTGF reporter activity after 24 h incubation. D. The chemical structure of K-975. Each bar or plot represents the mean (duplicate).

by micro-computed tomography (CT) imaging using a 3D micro-X-ray CT instrument for experimental animals (mCT2/FX; Rigaku, Tokyo, Japan). Iopamilone injection 370 (Bayer, Leverkusen, Germany), a nonionic radiocontrast agent for urography and angiography, was administered intravenously at 0.2 mL/head, and CT was started 5 to 10 min later. CT imaging data were analyzed using a dedicated software program (Rigaku).

Results

K-975 inhibits CTGF reporter activity in NCI-H661 cells

To identify an inhibitor of YAP1/TAZ-TEAD signaling, we screened the chemical libraries of Kyowa Kirin using CTGF reporter plasmid transfected NCI-H2052 cells, an NF2-deficient human MPM cell line, and NCI-H661 cells, a LATS1/2-deficient human NSCLC cell line. The CTGF promoter region contains a TEAD binding site [14]. When the YAP1 gene in NCI-H661/CTGF-Luc cells was knocked down by RNAi, a 60%-80% reduction in CTGF reporter gene activity was observed (**Figure 1A**). High-throughput screening identified some hit compounds. Through lead optimization, we synthesized K-975 as a small-molecule inhibitor of YAP1/TAZ-TEAD signaling (**Figure 1D**). K-975 strongly inhibited the reporter activity in NCI-H661/CTGF-Luc cells, and the maximum inhibition was approximately 70% (**Figure 1B**). In contrast, K-886, a derivative of K-975 with an acrylamide structure, did not inhibit the reporter activity in NCI-H661/CTGF-Luc cells. Neither compound inhibited the reporter activity in NCI-H661/NRF2-Luc cells used as a counter-screen

(**Figure 1C**). These results suggested that K-975 was an inhibitor of YAP1/TAZ-TEAD signaling.

K-975 inhibits YAP1/TAZ-TEAD PPI by binding to the PBP of TEAD

Crystallographic analysis of K-975 in complex with the TEAD1-YBD revealed that K-975 was covalently bound to Cys359 located in the PBP of TEAD1 via an acrylamide structure (**Figure 2A** and **2B**; **Table 1**). In addition, we performed SPR measurements using TEAD1-YBD and bio-YAPpep to evaluate the effect of K-975 on the PPI between TEAD1 and YAP1. In this assay system, an excess amount of YAPpep inhibits the YAP1-TEAD PPI. Using this assay system, we revealed that K-975 surely inhibited the YAP1-TEAD1 PPI (**Figure 2C**).

Next, we investigated whether K-975 inhibited the PPI between TEAD and YAP1 in cells using a Halo-tag pull-down assay. We evaluated the PPI between TEAD1 and YAP1 and between TEAD4 and YAP1 in NCI-H226 cells, an NF2-deficient MPM cell line. K-975 showed an inhibitory activity towards TEAD1-YAP1 PPI and TEAD4-YAP1 PPI as expected (**Figure 2D**). In addition, similar results were observed against TEAD1-TAZ PPI and TEAD4-TAZ PPI (**Figure 2E**). Furthermore, K-975 inhibited the palmitoylation of TEAD1-YBD (**Figure 2F**). K-886, which showed no inhibition in the CTGF-reporter assay, did not show any activity against YAP1/TAZ-TEAD PPI or the palmitoylation of TEAD1-YBD.

K-975 induces a similar gene expression profile to that of YAP1 siRNA and TEADs siRNA in NCI-H226 cells

To investigate whether K-975 selectively inhibited YAP1/TAZ-TEAD downstream signaling, we compared the effect of K-975 with YAP1 siRNA and/or TEADs siRNA on the expression profiles of YAP1-TEAD downstream genes. The knockdown efficacy of each siRNA at a concentration of 5 nmol/L for 48-h treatment is shown in **Figure 3A**. Each siRNA specifically inhibited its corresponding gene expression. As shown in **Figure 3B**, YAP1 siRNA and TEADs siRNA showed similar effects on the expression of *CTGF*, *IGFBP3*, *NPPB,* and *FBXO32* in NCI-H226 cells, all of which were identified as YAP1-TEAD downstream genes by microarray analysis performed in-house (data not shown). Interestingly, individual siRNAs for TEAD1, TEAD2, TEAD3, and TEAD4 did not induce a similar gene expression profile to YAP1 siRNA. This suggests there is compensation among the TEAD family members. Thus, the inhibition of all TEAD family members was necessary to inhibit YAP1-TEAD signaling.

Next, we evaluated the gene expression profile induced by K-975 in NCI-H226 cells. As with YAP1 siRNA and TEADs siRNA, K-975 decreased the expressions of *CTGF*, *IGFBP3,* and *NPPB* mRNAs, and increased the expression of *FBXO32* mRNA with 24-h treatment (**Figure 3C**). Therefore, we concluded that K-975 was a selective inhibitor of YAP1-TEAD signaling.

K-975 inhibits the cell proliferation of NF2-non-expressing mesothelioma cell lines

Next, we determined the inhibitory activity of K-975 against the proliferation of NF2-non-expressing MPM cell lines compared with NF2-expressing cell lines. First, the NF2 protein expression status was evaluated in a series of human MPM cell lines. As shown in **Figure 4B**, NCI-H226, Mero-14, Y-MESO-26B, Y-MESO-9, Y-MESO-28, NCI-H2052, and Y-MESO-14 were identified as NF2-non-expressing MPM cell lines. MSTO-211H, Mero-25, HMMME, NCI-H28, NCI-H2452, Y-MESO-27, and Y-MESO-30 were NF2-expressing MPM cell lines. Then, using these 14 MPM cell lines, cell proliferation assays were performed with K-975 incubated for 144 h. The findings in NF2-non-expressing cell lines are represented by solid lines and those of NF2-expressing cell lines are represented by dotted lines (**Figure 4A**). K-975 had a stronger inhibitory effect against NF2-non-expressing cell lines than NF2-expressing cell lines. K-975 also strongly inhibited the proliferation of MSTO-211H cells, an NF2-expressing cell line. This is because MSTO-211H cells express a LATS1-presenilin-1 (PSEN1) fusion gene that lacks the kinase activity of LATS1; therefore, YAP1/TAZ is constitutively activated in cells such as NF2-non-expressing cells [37].

K-975 exerts a significant anti-tumor effect by inhibiting YAP1/TAZ-TEAD signaling in s.c. transplant mouse models of human mesothelioma

Next, we investigated the anti-tumor effect of K-975 in SCID mice subcutaneously transplant-

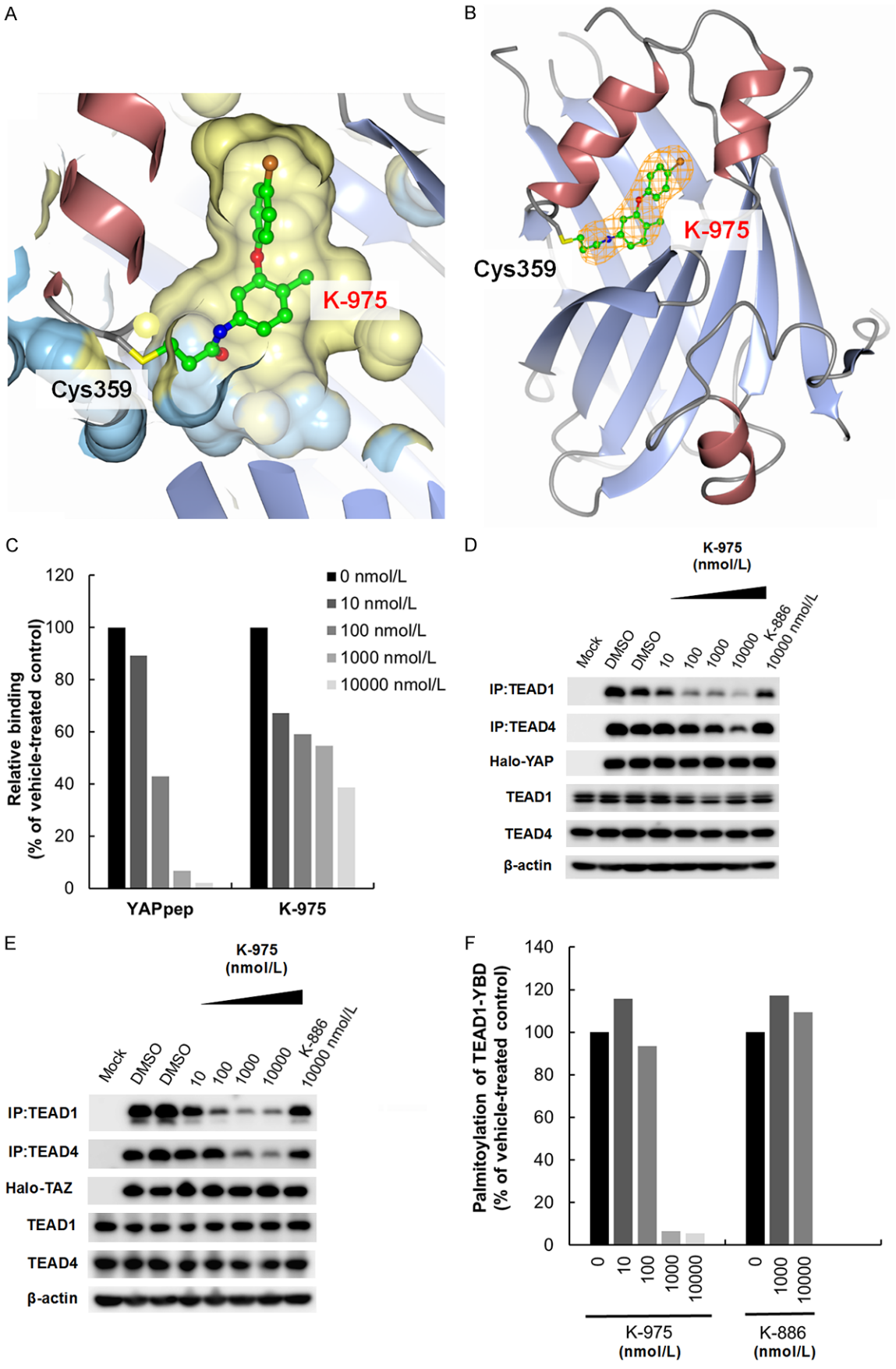
A
K-975
Cys359
B
K-975
Cys359
C
Relative binding (% of vehicle-treated control)
120
100
80
60
40
20
0
0 nmol/L
10 nmol/L
100 nmol/L
1000 nmol/L
10000 nmol/L
YAPpep
K-975
D
K-975 (nmol/L)
Mock
DMSO
DMSO
10
100
1000
10000
K-886 10000 nmol/L
IP:TEAD1
IP:TEAD4
Halo-YAP
TEAD1
TEAD4
β-actin
E
K-975 (nmol/L)
Mock
DMSO
DMSO
10
100
1000
10000
K-886 10000 nmol/L
IP:TEAD1
IP:TEAD4
Halo-TAZ
TEAD1
TEAD4
β-actin
F
Palmitoylation of TEAD1-YBD (% of vehicle-treated control)
140
120
100
80
60
40
20
0
0
10
100
1000
10000
K-975 (nmol/L)
0
1000
10000
K-886 (nmol/L)

Figure 2. K-975 binds to Cys359 of transcriptional enhanced associate domain 1 (TEAD1)-yes-associated protein 1-binding domain (YBD) directly and inhibits the protein-protein interaction (PPI) between yes-associated protein 1 (YAP1) and TEAD. A. The covalent binding of K-975 to TEAD1-YBD. TEAD1-YBD is shown as a "ribbon" model. K-975 and Cys359 are shown as "ball-and-stick" and "stick" models, respectively. The omit map (contoured at 3.0 σ) for K-975 is shown as orange mesh. B. Molecular surface of the binding pocket of K-975. Hydrophobic amino acids and polar amino acids are shown in light-yellow and light-blue, respectively. C. K-975 inhibited the PPI between TEAD1-YBD and biotinylated YAP1 peptide (bio-YAPpep). Bio-YAPpep was captured on a streptavidin-sensor chip, and the binding between TEAD1-YBD and bio-YAPpep was monitored with SPR equipment. D and E. K-975 exerted inhibitory activity against the PPI between (D) Halo-YAP and endogenous TEAD1/4 and (E) Halo-TAZ and TEAD1/4 in NCI-H226 cells after 24 h incubation. F. K-975 inhibited the auto-palmitoylation of TEAD1-YBD. The fluorescence intensities were normalized to the level of DMSO-treated TEAD1-YBD.

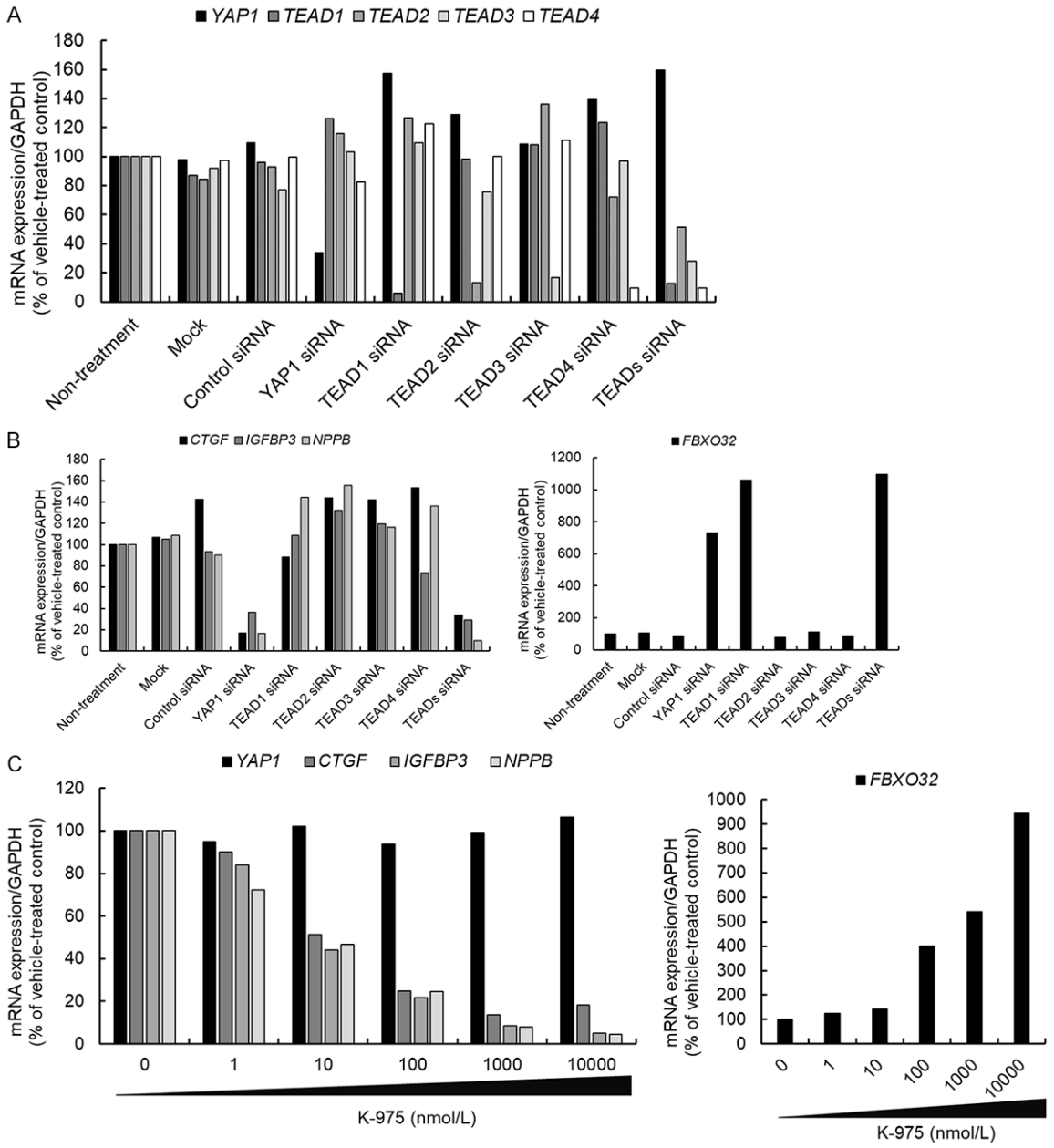

Figure 3. K-975 inhibits yes-associated protein 1 (YAP1)-transcriptional enhanced associate domain (TEAD) signaling by the same mechanism as YAP1 siRNA and TEADs siRNA. A. Knockdown efficacy of each siRNA after 48 h incubation. B. YAP1 siRNA and TEADs siRNA suppressed the mRNA expressions of *CTGF*, *IGFBP3,* and *NPPB*, and increased the mRNA expression of *FBXO32*. C. K-975 induced similar changes to the mRNA expression profile of YAP1-TEAD downstream genes after 24 h incubation. Each bar represents the mean (duplicate).

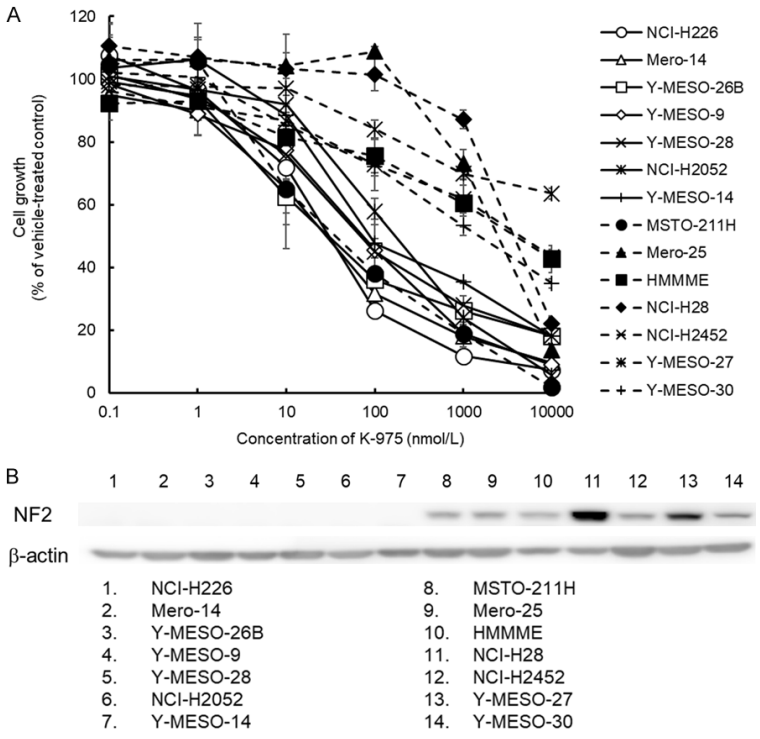

Figure 4. K-975 exerts a stronger inhibitory activity towards neurofibromin 2 (NF2)-non-expressing mesothelioma cell lines than NF2-expressing mesothelioma cell lines. A. K-975 inhibited the cell proliferation more potently in NF2-non-expressing cell lines (7 solid lines) than in NF2-expressing cell lines (7 dotted lines) after 144 h incubation. Each plot represents the mean ± SD (triplicate). B. NF2 protein expression in various human mesothelioma cell lines was evaluated by immunoblotting.

ed with NCI-H226 or MSTO-211H cells. K-975 was orally administered twice a day for 14 days at 10, 30, 100, and 300 mg/kg in the NCI-H226 s.c. xenograft model and at 30, 100, and 300 mg/kg in the MSTO-211H s.c. xenograft model. A strong anti-tumor effect of K-975 was observed in the MPM s.c. xenograft mouse models (**Figure 5A**, **5B**). The NCI-H226 s.c. xenograft model was resistant to monotherapy with PEM or CDDP. In contrast, the MSTO-211H s.c. xenograft model was sensitive to combination chemotherapy with PEM and CDDP, which is used as standard chemotherapy for malignant mesothelioma patients.

In addition, to determine whether K-975 inhibited YAP1-TEAD signaling *in vivo*, the gene expression profile in tumor tissues was analyzed. After the oral administration of K-975 twice a day for 3 days, the expressions of the same series of genes analyzed *in vitro* (**Figure 3C**) were determined by RT-PCR. K-975 decreased the expressions of *CTGF*, *IGFBP3,* and *NPPB* and increased the expression of *FBXO32* at 30-300 mg/kg in the NCI-H226 s.c. xenograft model (**Figure 5C**) and at 100-300 mg/kg in the MSTO-211H s.c. xenograft model (**Figure 5D**). Therefore, the anti-tumor effect of K-975 in the MPM s.c. xenograft mouse models was attributed to the inhibition of YAP1-TEAD signaling.

Combination therapy of K-975 and chemotherapy improves survival in an orthotopic transplant mouse model of human mesothelioma

Next, we examined whether the anti-tumor effect of K-975 prolonged the survival of nude mice orthotopically transplanted with NCI-H226 cells.

The group composition was as follows (treatment details for each group are shown in **Figure 5E**): Group 1, vehicle; Group 2, chemotherapy (PEM/CDDP); Group 3, K-975; and Group 4, combination of chemotherapy and K-975. For Groups 2 and 4, folic acid was also administered to reduce the toxicity caused by PEM. The drug treatment period was set from day 14 to day 34, and observation was continued without any drug treatment from day 35 to day 107.

On day 35, the day after the drug treatment period, tumor lesions in the thoracic cavity were detected by CT. As shown in **Figure 5F**, the tumor lesions tended to be smaller in the chemotherapy, K-975, and combination groups compared with the vehicle-treated group. Kaplan-Meier analysis revealed that the chemotherapy, K-975, and combination treatments prolonged survival compared with the vehicle-treated group (**Figure 5G**). The combination group had the greatest survival benefit among all groups.

K-975 exerts a synergistic effect with a CDK4/6 inhibitor in s.c. transplant mouse models of human mesothelioma

We evaluated the anti-tumor effect of the combination therapy of a CDK4/6 inhibitor (palboci-

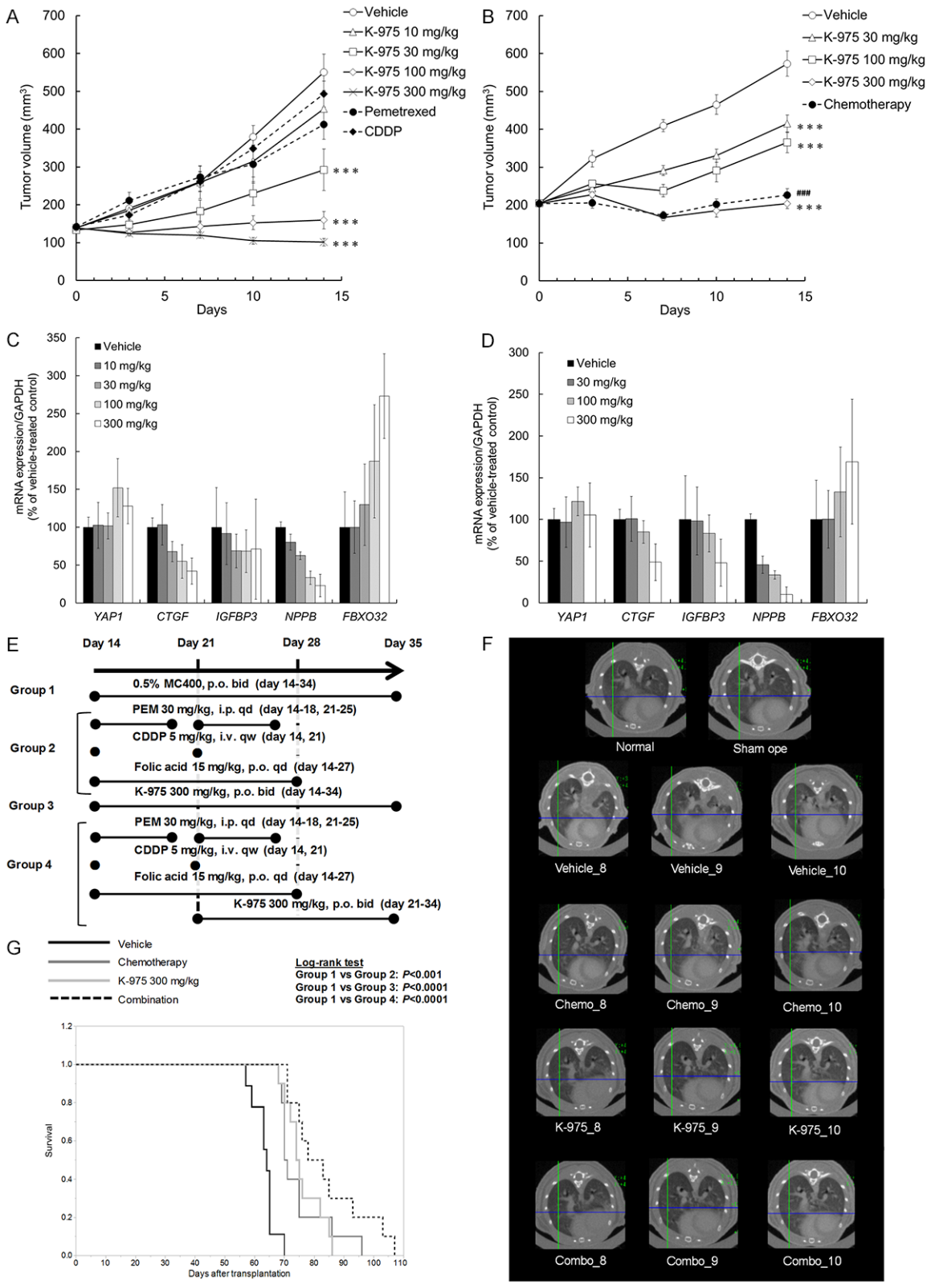

Figure 5. K-975 exerts an anti-tumor effect and significant survival benefit in human mesothelioma xenograft mice. A and B. K-975 suppressed the tumor growth in (A) NCI-H226 and (B) MSTO-211H xenograft models. Vehicle or K-975 was orally administered to mice twice a day for 14 days. Monotherapy of pemetrexed (PEM) (100 mg/kg, intraperitoneally (ip), once a day, daily) and cisplatin (CDDP) (5 mg/kg, intravenously (iv), once a day, weekly) or their combination (indicated as "chemotherapy": PEM [30 mg/kg, ip, once a day, 5 days-on/2 days-off] and CDDP [5 mg/

kg, iv, once a day, weekly]) was also administered to mice as a comparison. Each plot represents the mean ± SE (N = 5). ***: *P*<0.001 between the vehicle-treated group and K-975 30, 100, or 300 mg/kg-treated groups (analyzed by Williams test). ###: *P*<0.001 between the vehicle-treated group and chemotherapy (PEM, CDDP)-treated groups (analyzed by Student's *t*-test). C and D. K-975 inhibited yes-associated protein 1 (YAP1)-transcriptional enhanced associate domain (TEAD) signaling in (C) NCI-H226 and (D) MSTO-211H tumors. Each plot represents the mean ± SD (N = 5). E. The dosing schedule in the survival benefit evaluation of NCI-H226 orthotopic xenograft mice. F. Individual data of micro-computed tomography performed using the contrast agent Iopamiron. Tumors in the thoracic cavity were visualized on day 35. G. Survival curves were plotted by the Kaplan-Meier method, and the difference between the vehicle-treated group and each test group was analyzed by the Log-rank test. *P*<0.017 was regarded as statistically significant. Each group contained 10 mice, except for the vehicle-treated group, which contained 9 mice.

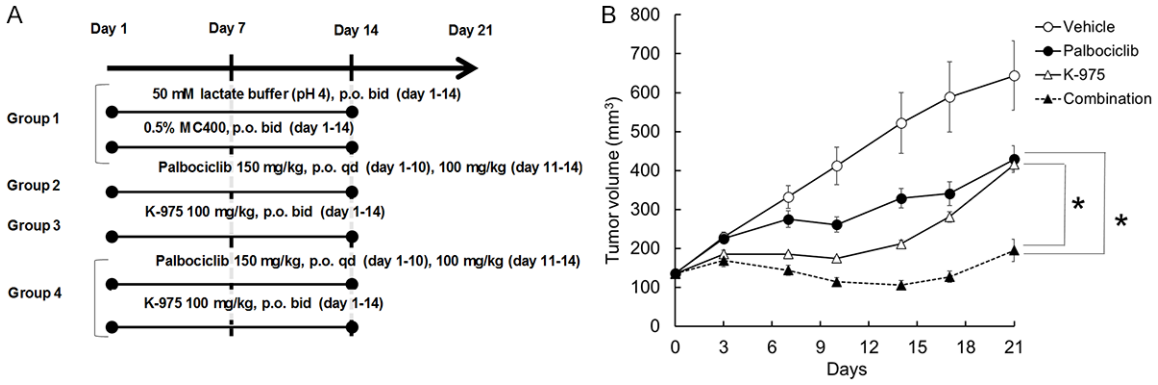

Figure 6. The combination of K-975 and a CDK4/6 inhibitor (palbociclib) synergistically suppressed tumor growth in human mesothelioma s.c. xenograft mice. A. The dosing schedule for the combination study in the NCI-H226 s.c. xenograft model. B. The anti-tumor effect of the combination of a CDK4/6 inhibitor and transcriptional enhanced associate domain (TEAD) inhibitor (▲) was more potent than that of each individual treatment (CDK4/6 inhibitor (palbociclib) (●), TEAD inhibitor (K-975) (Δ)). The tumor volume was monitored every 3-4 days. Each plot represents the mean ± SE of tumor volume (N = 5). *: *P*<0.05 between two selected groups on the final day of the experiment (analyzed by Tukey's test).

clib) and K-975 in the NCI-H226 s.c. xenograft model, deficient for NF2 and CDKN2A. The group composition was as follows (treatment details for each group are shown in **Figure 6A**): Group 1, vehicle; Group 2, palbociclib; Group 3, K-975; and Group 4, combination of palbociclib and K-975.

Our results showed that monotherapy with palbociclib or K-975 inhibited tumor growth compared with vehicle treatment, and that the combination group had the strongest anti-tumor effect among all groups (**Figure 6B**). The tumor volumes in the combination group on the last day of the study were significantly smaller than those in the monotherapy groups of each inhibitor (*P*<0.05). The body weight of mice in the combination group was not markedly different from that in the vehicle-treated group (data not shown). Consequently, the combination of a CDK4/6 inhibitor and K-975 was effective at enhancing the anti-tumor effect against MPM.

Discussion

In this study, we used the CTGF reporter screening system to identify K-975 as an inhibitor of YAP1/TAZ-TEAD signaling (**Figure 1B**). By investigating the mechanism of action of K-975, we found that it directly bound to a Cys residue located in the PBP of TEAD1-YBD in a covalent manner (**Figure 2A**, **2B**). Although there have been some reports of covalent inhibitors against YAP1/TAZ-TEAD PPI, the inhibitory activities of these compounds were poor in cell-based assays [38, 39]. Our newly identified TEAD inhibitor K-975 exerted strong inhibitory activity against YAP1/TAZ-TEAD PPI (**Figure 2D**, **2E**), resulting in the inhibition of the downstream signaling factors (**Figure 3C**) at double-digit nanomolar concentrations in human MPM cells.

In **Figure 2D**, **2E**, pull-down assays were performed with TEAD1 and TEAD4; however, K-975

is expected to exert the same inhibitory effect against TEAD2 and TEAD3, because the Cys residue to which K-975 binds is conserved in all TEAD family members. Furthermore, in **Figure 3B**, the knockdown of all TEAD family members showed the same gene signature as YAP1 knockdown in contrast to the individual knockdown of each TEAD member. K-975 induced the same effect on the gene expression profile as that induced by the combination of TEAD1, 2, 3, and 4 siRNAs (**Figure 3C**). Consequently, K-975 is considered a pan-TEAD inhibitor.

Bum-Erdene et al. used TED-347, which binds covalently to the Cys residue in the PBP of TEAD, and reported that the inhibition of palmitoylation induced conformational changes in TEAD, mainly in the PPI interface with YAP1/TAZ, and that this new conformation was not suitable for binding to YAP1/TAZ [39]. Because K-975 binds to the same Cys residue and also inhibits the palmitoylation of TEAD (**Figure 2A**, **2B**, **2F**), a similar conformational change might be induced by K-975. In contrast, in the SPR assay (**Figure 2C**), K-975 inhibited the PPI between YAP1 and TEAD1-YBD, which had not been palmitoylated. Therefore, K-975 inhibited YAP1-TEAD PPI via its own binding without affecting the palmitoylation status of TEAD indicating K-975 induces conformational changes in the TEAD protein directly, leading to the inhibition of YAP1/TAZ binding in an allosteric manner. The activity of K-975 was greater in the cell-based assay (**Figures 2D**, **2E**, **3C**) than in the cell-free assay (**Figure 2C**, **2F**). This might be explained by two conformational changes-one induced by the inhibition of palmitoylation and the other induced in an allosteric manner-that contribute to the cellular activity of K-975. To clarify the mechanism of action of K-975 in greater detail, further experiments will be needed.

K-975 had a greater inhibitory effect towards the proliferation of NF2-non-expressing human MPM cell lines compared with NF2-expressing MPM cell lines (**Figure 4**). Because the gene alteration of NF2 is relatively common in malignant mesothelioma patients [19, 20], this suggests that NF2 may be a predictive biomarker in future clinical trials of malignant mesothelioma patients. However, the gene alteration of NF2 is not as common in other human cancers [40]. Therefore, other gene alterations of Hippo pathway molecules, such as the activation status of YAP1/TAZ, should be assessed as potential predictive biomarkers that can be used across cancer types.

K-975 inhibited tumor growth by suppressing the downstream signaling of the YAP1/TAZ-TEAD complex in mice subcutaneously transplanted with human MPM cells with gene alterations in certain Hippo pathway molecules (either NF2-deficient or with the LATS1-PSEN1 fusion gene) (**Figure 5A-D**). The anti-tumor effect of K-975 was greater than that of the combination chemotherapy of PEM and CDDP. In addition, the greatest survival benefit was observed by a combination of K-975 and chemotherapy in mice orthotopically transplanted with NF2-deficient MPM cells (**Figure 5G**). Based on these results, K-975 is expected to be an effective therapeutic agent for MPM patients with gene alterations in the Hippo pathway.

Furthermore, when K-975 was administered with the CDK4/6 inhibitor palbociclib to the NF2-deficient MPM s.c. xenograft mice model, the anti-tumor effect was significantly enhanced compared with the monotherapy of K-975 or palbociclib (**Figure 6B**). In malignant mesothelioma, the frequency of NF2 mutation and/or deficiency is about 40%-50%, that of CDKN2A/B deficiency is about 35%-70%, and that of CDKN2A mutation is about 5%-10% [29]. These genetic alterations are not mutually exclusive. Therefore, a certain percentage of malignant mesothelioma patients who might benefit from K-975 likely have both NF2 mutation/deficiency and CDKN2A/B mutation/deficiency.

K-975 did not cause any severe toxicities, such as body weight loss or death, at least in the mouse models used in this study. However, because the Hippo pathway is a key pathway in development, the use of inhibitors against YAP1/TAZ-TEAD signaling should be avoided in young children and/or pregnant women. Furthermore, even in adult tissues, there is some concern regarding the safety of inhibiting YAP1/TAZ-TEAD signaling. Indeed, we observed pathological findings suggesting proteinuria in rats and monkeys after a two-week treatment with our drug candidate, a derivative of K-975 that shows a better metabolic profile [41]. Several other reports have also described toxicity caused by the inhibition of YAP1/TAZ-TEAD in many tissues, including the heart, liver, kid-

ney, and nervous system [42-44]. Therefore, the safety profile should be determined carefully to ensure the optimal usage of TEAD inhibitors in clinical settings.

In recent years, the development of drugs targeting Hippo pathway molecules, especially the YAP1/TAZ-TEAD transcription complex, has been vigorously pursued. However, few inhibitors of YAP1/TAZ-TEAD PPI have achieved strong activity and high selectivity. Our newly identified TEAD inhibitor K-975 shows strong activity and high selectivity, suggesting its potential as an effective drug candidate for MPM therapy.

Acknowledgements

The authors thank Miyoko Suzuki, Kumiko Masunaga, Etsuko Koshimura, and Akiko Katsumata for their excellent technical assistance. This work was funded by Kyowa Kirin Co., Ltd.

Disclosure of conflict of interest

None.

Address correspondence to: Ayumi Kaneda, R&D Division, Kyowa Kirin Co., Ltd., 1188 Shimotogari, Nagaizumi-cho, Sunto-gun, Shizuoka, 411-8731, Japan. Tel: +81-55-989-4488; Fax: +81-55-986-7430; E-mail: ayumi.kaneda.s4@kyowakirin.com

References

[1] Huang J, Wu S, Barrera J, Matthews K and Pan D. The Hippo signaling pathway coordinately regulates cell proliferation and apoptosis by inactivating Yorkie, the Drosophila homolog of YAP. Cell 2005; 122: 421-434.

[2] Oh H and Irvine KD. Yorkie: the final destination of Hippo signaling. Trends Cell Biol 2010; 20: 410-417.

[3] Piccolo S, Dupont S and Cordenonsi M. The biology of YAP/TAZ: hippo signaling and beyond. Physiol Rev 2014; 94: 1287-1312.

[4] Yu FX, Zhao B and Guan KL. Hippo pathway in organ size control, tissue homeostasis, and cancer. Cell 2015; 163: 811-828.

[5] Calses PC, Crawford JJ, Lill JR and Dey A. Hippo pathway in cancer: aberrant regulation and therapeutic opportunities. Trends Cancer 2019; 5: 297-307.

[6] Pobbati AV, Han X, Hung AW, Weiguang S, Huda N, Chen GY, Kang C, Chia CS, Luo X, Hong W and Poulsen A. Targeting the central pocket in human transcription factor TEAD as a potential cancer therapeutic strategy. Structure 2015; 23: 2076-2086.

[7] Holden JK and Cunningham CN. Targeting the Hippo pathway and cancer through the TEAD family of transcription factors. Cancers (Basel) 2018; 10: 81.

[8] Li Z, Zhao B, Wang P, Chen F, Dong Z, Yang H, Guan KL and Xu Y. Structural insights into the YAP and TEAD complex. Genes Dev 2010; 24: 235-240.

[9] Chan P, Han X, Zheng B, DeRan M, Yu J, Jarugumilli GK, Deng H, Pan D, Luo X and Wu X. Autopalmitoylation of TEAD proteins regulates transcriptional output of the Hippo pathway. Nat Chem Biol 2016; 12: 282-289.

[10] Noland CL, Gierke S, Schnier PD, Murray J, Sandoval WN, Sagolla M, Dey A, Hannoush RN, Fairbrother WJ and Cunningham CN. Palmitoylation of TEAD transcription factors is required for their stability and function in Hippo pathway signaling. Structure 2016; 24: 179-186.

[11] Zhao B, Ye X, Yu J, Li L, Li W, Li S, Yu J, Lin JD, Wang CY, Chinnaiyan AM, Lai ZC and Guan KL. TEAD mediates YAP-dependent gene induction and growth control. Genes Dev 2008; 22: 1962-1971.

[12] Chen YA, Lu CY, Cheng TY, Pan SH, Chen HF and Chang NS. WW domain-containing proteins YAP and TAZ in the Hippo pathway as key regulators in stemness maintenance, tissue homeostasis, and tumorigenesis. Front Oncol 2019; 9: 60.

[13] Zhou Y, Huang T, Cheng AS, Yu J, Kang W and To KF. The TEAD family and its oncogenic role in promoting tumorigenesis. Int J Mol Sci 2016; 17: 138.

[14] Fujii M, Toyoda T, Nakanishi H, Yatabe Y, Sato A, Matsudaira Y, Ito H, Murakami H, Kondo Y, Kondo E, Hida T, Tsujimura T, Osada H and Sekido Y. TGF-β synergizes with defects in the Hippo pathway to stimulate human malignant mesothelioma growth. J Exp Med 2012; 209: 479-494.

[15] Zhang X, George J, Deb S, Degoutin JL, Takano EA and Fox SB; AOCS Study group, Bowtell DD and Harvey KF. The Hippo pathway transcriptional co-activator, YAP, is an ovarian cancer oncogene. Oncogene 2011; 30: 2810-2822.

[16] Hua G, Lv X, He C, Remmenga SW, Rodabough KJ, Dong J, Yang L, Lele SM, Yang P, Zhou J, Karst A, Drapkin RI, Davis JS and Wang C. YAP induces high-grade serous carcinoma in fallopian tube secretory epithelial cells. Oncogene 2016; 35: 2247-2265.

[17] Pei T, Li Y, Wang J, Wang H, Liang Y, Shi H, Sun B, Yin D, Sun J, Song R, Pan S, Sun Y, Jiang H, Zheng T and Liu L. YAP is a critical oncogene in human cholangiocarcinoma. Oncotarget 2015; 6: 17206-17220.

[18] Marti P, Stein C, Blumer T, Abraham Y, Dill MT, Pikiolek M, Orsini V, Jurisic G, Megel P, Makowska Z, Agarinis C, Tornillo L, Bouwmeester T, Ruffner H, Bauer A, Parker CN, Schmelzle T, Terracciano LM, Heim MH and Tchorz JS. YAP promotes proliferation, chemoresistance, and angiogenesis in human cholangiocarcinoma through TEAD transcription factors. Hepatology 2015; 62: 1497-1510.

[19] Woodard GA, Yang YL, You L and Jablons DM. Drug development against the Hippo pathway in mesothelioma. Transl Lung Cancer Res 2017; 6: 335-342.

[20] Sekido Y. Molecular pathogenesis of malignant mesothelioma. Carcinogenesis 2013; 34: 1413-1419.

[21] Moroishi T, Hansen CG and Guan KL. The emerging roles of YAP and TAZ in cancer. Nat Rev Cancer 2015; 15: 73-79.

[22] Liu H, Du S, Lei T, Wang H, He X, Tong R and Wang Y. Multifaceted regulation and functions of YAP/TAZ in tumors (Review). Oncol Rep 2018; 40: 16-28.

[23] Scherpereel A, Mazieres J, Greillier L, Lantuejoul S, Dô P, Bylicki O, Monnet I, Corre R, Audigier-Valette C, Locatelli-Sanchez M, Molinier O, Guisier F, Urban T, Ligeza-Poisson C, Planchard D, Amour E, Morin F, Moro-Sibilot D and Zalcman G; French Cooperative Thoracic Intergroup. Nivolumab or nivolumab plus ipilimumab in patients with relapsed malignant pleural mesothelioma (IFCT-1501 MAPS2): a multicentre, open-label, randomised, non-comparative, phase 2 trial. Lancet Oncol 2019; 20: 239-253.

[24] Forde PM, Scherpereel A and Tsao AS. Use of immune checkpoint inhibitors in mesothelioma. Curr Treat Options Oncol 2019; 20: 18.

[25] Kandoussi I, Lakhlili W, Taoufik J and Ibrahimi A. Docking analysis of verteporfin with YAP WW domain. Bioinformation 2017; 13: 237-240.

[26] Crawford JJ, Bronner SM and Zbieg JR. Hippo pathway inhibition by blocking the YAP/TAZ-TEAD interface: a patent review. Expert Opin Ther Pat 2018; 28: 867-873.

[27] Tang TT, Konradi AW, Feng Y, Peng X, Qiao S and Post L. Abstract 2693: targeting the Hippo-YAP pathway with novel small-molecule inhibitors of the YAP-TEAD transcription activity. AACR Annual Meeting 2019, Atlanta, Georgia.

[28] Jiao S, Wang H, Shi Z, Dong A, Zhang W, Song X, He F, Wang Y, Zhang Z, Wang W, Wang X, Guo T, Li P, Zhao Y, Ji H, Zhang L and Zhou Z. A peptide mimicking VGLL4 function acts as a YAP antagonist therapy against gastric cancer. Cancer Cell 2014; 25: 166-180.

[29] Kato S, Tomson BN, Buys TP, Elkin SK, Carter JL and Kurzrock R. Genomic landscape of malignant mesotheliomas. Mol Cancer Ther 2016; 15: 2498-2507

[30] Bonelli MA, Digiacomo G, Fumarola C, Alfieri R, Quaini F, Falco A, Madeddu D, La Monica S, Cretella D, Ravelli A, Ulivi P, Tebaldi M, Calistri D, Delmonte A, Ampollini L, Carbognani P, Tiseo M, Cavazzoni A and Petronini PG. Combined inhibition of CDK4/6 and PI3K/AKT/mTOR pathways induces a synergistic anti-tumor effect in malignant pleural mesothelioma cells. Neoplasia 2017; 19: 637-648.

[31] Kabsch W. XDS. Acta Crystallogr D Biol Crystallogr 2010; 66: 125-132.

[32] Vagin A and Teplyakov A. MOLREP: an automated program for molecular replacement. J Appl Cryst 1997; 30: 1022-1025.

[33] Collaborative Computational Project, Number 4. The CCP4 suite: programs for protein crystallography. Acta Crystallogr D Biol Crystallogr 1994; 50: 760-763.

[34] Murshudov GN, Vagin AA and Dodson EJ. Refinement of macromolecular structures by the maximum-likelihood method. Acta Crystallogr D Biol Crystallogr 1997; 53: 240-255.

[35] Emsley P, Lohkamp B, Scott WG and Cowtan K. Features and development of Coot. Acta Crystallogr D Biol Crystallogr 2010; 66: 486-501.

[36] McNicholas S, Potterton E, Wilson KS and Noble ME. Presenting your structures: the CCP-4mg molecular-graphics software. Acta Crystallogr D Biol Crystallogr 2011; 67: 386-394.

[37] Miyanaga A, Masuda M, Tsuta K, Kawasaki K, Nakamura Y, Sakuma T, Asamura H, Gemma A and Yamada T. Hippo pathway gene mutations in malignant mesothelioma: revealed by RNA and targeted exon sequencing. J Thorac Oncol 2015; 10: 844-851.

[38] Lu W, Wang J, Li Y, Tao H, Xiong H, Lian F, Gao J, Ma H, Lu T, Zhang D, Ye X, Ding H, Yue L, Zhang Y, Tang H, Zhang N, Yang Y, Jiang H, Chen K, Zhou B and Luo C. Discovery and biological evaluation of vinylsulfonamide derivatives as highly potent, covalent TEAD autopalmitoylation inhibitors. Eur J Med Chem 2019; 184: 111767.

[39] Bum-Erdene K, Zhou D, Gonzalez-Gutierrez G, Ghozayel MK, Si Y, Xu D, Shannon HE, Bailey BJ, Corson TW, Pollok KE, Wells CD and Meroueh SO. Small-molecule covalent modification of conserved cysteine leads to allosteric inhibition of the TEAD·Yap protein-protein interaction. Cell Chem Biol 2019; 26: 378-389.

[40] Petrilli AM and Fernández-Valle C. Role of Merlin/NF2 inactivation in tumor biology. Oncogene 2016; 35: 537-548.

[41] Kaneda A, Seike T, Uemori T, Myojo K, Aida K, Danjo T, Nakajima T, Yamaguchi D, Hamada T, Tsuji Y, Hamaguchi K, Yasunaga M, Otsubo N, Onodera H, Nishiya Y, Suzuki M, Saito J, Ishii T and Nakai R. Abstract 3086: discovery of a first-in-class TEAD inhibitor which directly inhibits YAP/TAZ-TEAD protein-protein interac-

tion and shows a potent anti-tumor effect in malignant pleural mesothelioma. AACR Annual Meeting 2019, Atlanta, Georgia.
[42] Kodaka M and Hata Y. The mammalian Hippo pathway: regulation and function of YAP1 and TAZ. Cell Mol Life Sci 2015; 72: 285-306.
[43] Wong JS, Meliambro K, Ray J and Campbell KN. Hippo signaling in the kidney: the good and the bad. Am J Physiol Renal Physiol 2016; 311: F241-8.
[44] Kakiuchi-Kiyota S, Schutten MM, Zhong Y, Crawford JJ and Dey A. Safety considerations in the development of Hippo pathway inhibitors in cancers. Front Cell Dev Biol 2019; 7: 156.